Valence-band Auger-electron spectra for aluminum

J. W. Gadzuk
National Bureau of Standards, Washington, D.C. 20234
(Received 14 August 1973)

Recent measurements of the L_{23}VV auger spectrum of Al by Powell, have shown that the observed energy distributions do not correspond to the self-convolution of the Al bulk density of states. Attempts to account for this discrepancy in terms of energy-dependent matrix elements and inelastic scattering of the ejected electron are described here.

Powell[1] has observed the Auger spectrum of the L_{23}VV transitions in Al for electrons which are ejected into a small solid angle centered ~60° from the normal to the surface. For such an Auger transition, it was expected that the energy distribution would be similar to the self-convolution of the conduction-band density of states,[2,3]

$$N'(2\xi - \epsilon_C) = (\gamma/\alpha^2)\int_0^{\xi_u} d\Delta\, \rho(\xi+\Delta)\rho(\xi-\Delta) \qquad (1)$$

with γ/α^2 some constants, $\rho(\xi)$ the band density of states, $2\xi - \epsilon_C$ the final-state energy, and $\xi_u = \xi$ if $\xi < \frac{1}{2}\epsilon_B$ or $\xi_u = \epsilon_B - \xi$ if $\xi > \frac{1}{2}\epsilon_B$. In the case of the free-electron gas which is a reasonable model for Al, $\rho(\xi) = \alpha\xi^{1/2}$. The relevant energy-level diagram for the L_{23}VV transition and the form of the energy distribution are shown in Fig. 1. Here energies are referenced with respect to a zero at the bottom of the band. The Fermi level is at ϵ_B and the core level at ϵ_C with ϵ_C a negative number. Within this convention, the core-electron binding energy as usually defined would equal $\epsilon_B - \epsilon_C$. The experimental results of Powell indicate that the maximum in $N'(2\xi - \epsilon_C)$ falls at an energy ~5 eV above the maximum predicted by folding the Al density of states into itself, suggesting that either matrix element and/or surface effects cannot be neglected, as they have been in Eq. (1). In either case, some mechanism is required which overly emphasizes the role of the higher-energy initial states ϵ_1 and ϵ_2 in the Auger process. To date, only limited theoretical work has been done on Auger transitions involving valence states.[4-9]

First the energy dependence of the matrix element for volume Auger production was considered as a possible source of correction. The customary[10] two-electron Auger matrix element was evaluated following the theory of Joyes and co-workers.[4,5] Without going into details here, the net result of using an energy-dependent matrix element was that the theoretical energy distribution then had a maximum which was slightly shifted (~0.5 eV) towards lower energies. However, this effect is comparatively small and will henceforth be neglected.

As a consequence of inelastic attenuation[11-13] of the final-state electrons, the unscattered electrons which are ejected must originate from a region very close to the surface. In fact in the energy range 50–70 eV above the Fermi level, the theoretical energy-dependent mean free path l_e is near its minimum value[11,14] of ~3 Å. All low-energy-electron-diffraction (LEED) analyses[15] of Al agree that a value of $l_e \simeq 4$ Å is approximately the correct result at these values of energy. The Al overlayer experiments of Tracy[16] suggest a somewhat smaller value of $l_e \approx 3$ Å. To include the influence of electron attenuation on the L_{23}VV spectrum, as a first approximation Eq. (1), the self-convolution of the bulk density of states is replaced by

$$N'(2\xi - \epsilon_C) \sim (\gamma/\alpha^2)\int_0^{-\infty} dz\, e^{\kappa z} \times \int_0^{\xi_u} d\Delta \rho(\xi+\Delta; z)\rho(\xi-\Delta; z), \qquad (2)$$

where the metal is assumed to occupy the semi-infinite half-space $z \le 0$ with z normal to the sur-

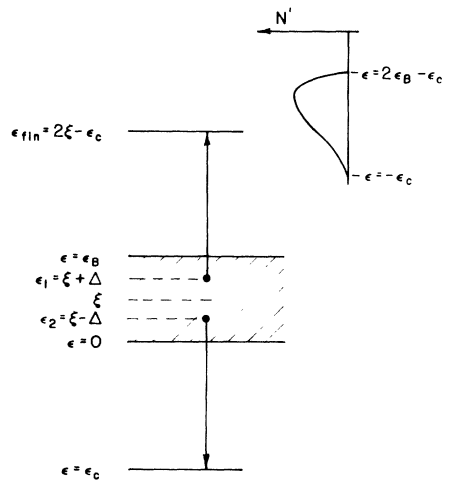

FIG. 1. Energy-level diagram depicting a CVV auger transition. The cross-hatched area is the occupied portion of the conduction band and the Fermi level is at $\epsilon = \epsilon_B$. Also shown is the resulting energy distribution.

face, $\rho(\xi; z)$ is the local density of states at z, $\kappa \equiv 1/l_e \times \cos\theta$, θ is the angle between the electron trajectory and the surface normal (which in the experiment of Powell was $\sim 60°$ neglecting refraction effects at the surface), and l_e is the total effective mean free path.

The local density of states is given by

$$\rho(\xi; z) = \sum_{\vec{k}} \int |\Psi_{\vec{k}}(\vec{r}_T; z)|^2 d^2 r_T \, \delta(\xi - \epsilon(\vec{k})),$$

where $\Psi_{\vec{k}}(\vec{r}_T, z)$ is the electron wave function, $\epsilon(\vec{k}) = (\hbar^2/2m)(k_T^2 + k_z^2)$, k_T is the wave vector in the transverse direction, the r_T integration averages the integrand over all the surface, and the sum is over all states $\vec{k}$ on the constant energy surface. For simplicity sine wave functions are used in the z direction so

$$\Psi_{\vec{k}}(\vec{r}_T, z) = (2/\Omega)^{1/2} \sin k_z z \, e^{i\vec{k}_T \cdot \vec{r}_T}, \tag{3}$$

with Ω the volume of the crystal. Using Eq. (3) in Eq. (2) and converting the sum to an integral, it is a simple exercise to show that the local density of states is given by

$$\rho(\xi; z) = \alpha \xi^{1/2} [1 - \sin 2k(\xi) z / 2k(\xi) z] \tag{4}$$

with $k(\xi) = [(2m/\hbar^2)\xi]^{1/2}$ and $\alpha \xi^{1/2} = \rho(\xi)$, the bulk density of states. The important feature of Eq. (4) is that for small z, $\rho(\xi; z) \sim \rho(\xi) \xi z^2$ and in this region, for a given z, the states of higher ξ are weighted more heavily than those of lower ξ in the bottom part of the band as contrasted to their weighting in the bulk. This is just the type of mechanism demanded by the Powell data. Inserting Eq. (4) into Eq. (2) twice, once for $\xi + \Delta$ and once for $\xi - \Delta$, and performing the z integration,[17] the resulting energy distribution is

$$N'(2\xi - \epsilon_C) \sim \int_0^{\xi_u} d\Delta \, k_+ k_- \left[1 - \frac{\kappa}{2k_+} \tan^{-1}\left(\frac{2k_+}{\kappa}\right) - \frac{\kappa}{2k_-} \tan^{-1}\left(\frac{2k_-}{\kappa}\right) + \frac{\kappa}{4k_-} \tan^{-1}\left(\frac{4k_-\kappa}{\kappa^2 + 4k_+^2 - 4k_-^2}\right) \right.$$
$$\left. + \frac{\kappa}{4k_+} \tan^{-1}\left(\frac{4k_+\kappa}{\kappa^2 + 4k_-^2 - 4k_+^2}\right) - \frac{\kappa^2}{16 k_+ k_-} \ln\left(\frac{\kappa^2 + 4(k_+ + k_-)^2}{\kappa^2 + 4(k_+ - k_-)^2}\right) \right]. \tag{5}$$

where $k_\pm = [(2m/\hbar^2)(\xi \pm \Delta)]^{1/2}$. Equation (5) has been numerically integrated treating $l_e = 2/\kappa$ (i.e., $\cos\theta = \frac{1}{2}$) parametrically, taking $\epsilon_B = 11.6$ eV, $\epsilon_C = -61.4$ eV (-73 eV with respect to the Fermi level), and the resulting normalized $N'(2\xi - \epsilon_C)$ vs 2ξ curves are shown in Fig. 2. The curve labeled $\rho * \rho$ is the bulk expression given by Eq. (5) with $\kappa \to 0$. The curve labeled Expt. is the experimental curve due to Powell.[1] As l_e decreases, the peak position in the energy distribution moves higher in energy towards the experimental curve. This is due to the greater weighting of high-energy states as the unscattered electrons originate closer to the surface.

Although the sign of the peak shift due to surface localization is correct, no curve which was calculated using a realistic value for l_e yielded a peak shift large enough to fully account for the experimental results. However, the restrictive choice of sine waves rather than more realistic wave functions affects the results adversely. The total local charge density, obtained by integrating Eq. (4) on energy from $\xi = 0$ to $\xi = \epsilon_B$, rises from zero at $z = 0$ to its internal value in a distance $\sim 0.2\lambda_F$, where λ_F is the Fermi wavelength. The local charge density obtained from the self-consistent jellium calculations of Lang[18] is qualitatively similar to the integrated Eq. (4), although the surface boundary conditions are not as stringent as in the infinite square well. The consequence is that the local charge density increase from zero to the internal value occurs over a distance $\sim 0.4\lambda_F$. The role of the mean free path is to favor the region of small z and thus rising charge density as the source region of unscattered electrons. Since this inhomogeneous region, in the sine wave case, is only $\sim \frac{1}{2}$ the thickness of the region in the self-

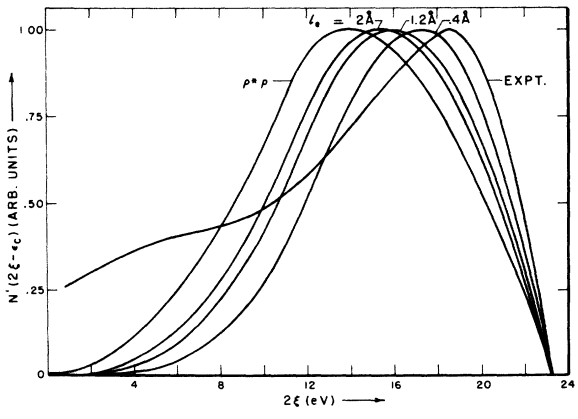

FIG. 2. Al L_{23} VV auger spectrum under various conditions. The curve labeled $\rho * \rho$ is the self-convolution of the free-electron density of states. Expt. is the experimentally determined spectrum (Ref. 1). The curves labeled with values of l_e are calculated from Eq. (5). The energy scale runs from $2\xi = 0$ to $2\xi = 2\epsilon_B = 23.2$ eV.

consistent case, an attenuation length of $\sim\frac{1}{2}$ the realistic value is required to achieve equivalent surface localization. On this basis N' from Eq. (5), with $l_e \simeq 1.5$ Å, should be most representative of a true energy distribution from a sample with $l_e = 3$ Å. Allowing for this correction, the surface localization accounts for about half the peak shift. Perhaps, other matrix element effects which are present in the surface region but not in the bulk, are responsible for the additional peak shift.

Last, it should be pointed out that the experimental curve, as drawn in Fig. 2, is a result of subtracting a plausible but arbitrary background from the raw data. Other choices of background subtraction could shift the peak downwards by as much as 1 eV. The steep rise ~10–15 eV below threshold has been postulated[1] to be due to electrons inelastically scattered from surface or bulk plasmons. Since this portion of the inelastic background has not been removed from the data, the theoretical and experimental curves are not expected to coincide on the low-energy side.

The assistance and helpful discussion with Dr. C. J. Powell is gratefully acknowledged.

[1]C. J. Powell, Phys. Rev. Lett. 30, 1179 (1973).
[2]J. J. Lander, Phys. Rev. 91, 1382 (1953).
[3]H. D. Hagstrum, Science 178, 275 (1972).
[4]P. Joyes and J. F. Hennequin, J. Phys. (Paris) 29, 483 (1968).
[5]M. Natta and P. Joyes, J. Phys. Chem. Solids 31, 447 (1970).
[6]V. Heine, Phys. Rev. 151, 561 (1966).
[7]B. W. Holland, L. McDonnell, and D. P. Woodruff, Solid State Commun. 11, 991 (1972).
[8]P. J. Feibelman, Phys. Rev. B 7, 2305 (1973).
[9]P. J. Feibelman, Surface Sci. 36, 558 (1973).
[10]E. H. S. Burhop, Adv. At. Mol. Phys. 8, 163 (1972).
[11]J. J. Quinn, Phys. Rev. 126, 1453 (1962).
[12]S. Q. Wang and G. D. Mahan, Phys. Rev. B 6, 4517 (1972).
[13]G. D. Mahan, Phys. Status Solidi (b) 55, 703 (1973).
[14]R. H. Ritchie, F. W. Garber, M. Y. Nakai, and R. D. Birkhoff, in *Advances in Radiation Biology*, edited by L. G. Augenstein, R. Mason, and M. Zelle (Academic, New York, 1969), Vol. 3.
[15]C. B. Duke and C. Tucker, Surface Sci. 15, 231 (1969); 19, 117 (1970); S. Y. Tong and T. N. Rhodin, Phys. Rev. Lett. 26, 711 (1971); G. Laramore and C. B. Duke, Phys. Rev. B 5, 267 (1972); D. W. Jepson, P. M. Marcus, and F. Jona, Phys. Rev. B 5, 3933 (1972); B 6, 3684 (1972); M. R. Martin and G. A. Somorjai, Phys. Rev. B 7, 3607 (1973).
[16]J. C. Tracy, J. Vac. Sci. Technol. (to be published).
[17]G. E. Roberts and H. Kaufman, *Table of Laplace Transforms* (W. B. Saunders, Philadelphia, 1966), p. 31.
[18]N. D. Lang, Solid State Commun. 7, 1037 (1969).